Lawrence Berkeley National Laboratory
LBL Publications

Title
Au+Au reactions at the AGS: Experiments E866 and E917

Permalink
https://escholarship.org/uc/item/32k6p2vj

Journal
Nuclear Physics A, 638(1-2)

ISSN
0375-9474

Authors
Ogilvie, CA
Ahle, L
Akiba, Y
et al.

Publication Date
1998-08-01

DOI
10.1016/s0375-9474(98)00388-1

Peer reviewed

Au+Au Reactions at the AGS: Experiments E866 and E917

C.A. Ogilvie for the E866 and E917 Collaborations [a]

[a]Department of Physics, MIT, Cambridge, MA 02139, USA

E866 Collaboration
L.Ahle[9], Y.Akiba[6], K.Ashktorab[2], M.D.Baker[9], D.Beavis[2], H.C.Britt[8], J.Chang[4], C.Chasman[2], Z.Chen[2], Y.Y.Chu[2], T.Chujo[11], V.Cianciolo[16], B.A.Cole[17], H.J.Crawford[3], J.B.Cumming[2], R.Debbe[2], J.C.Dunlop[9], W.Eldredge[4], J.Engelage[3], S.-Y.Fung[4], E.Garcia[13], S.Gushue[2], H.Hamagaki[15], L. Hansen[8], R.S.Hayano[10], G.Heintzelman[9], E.Judd[3], J.Kang[12], E.-J.Kim[12], A.Kumagai[11], K.Kurita[11], J.-H.Lee[2], J.Luke[8], Y.Miake[11], A.Mignerey[13], B.Moskowitz[2], M.Moulson[17], C.Muentz[2], S.Nagamiya[5], K.Nagano[10], M.N.Namboodiri[8], C.A.Ogilvie[9], J.Olness[2], K. Oyama[10], L.P.Remsberg[2], H.Sako[11], T.C.Sangster[8], R.Seto[4], J.Shea[13], K.Shigaki[2], R.Soltz[8], S.G.Steadman[9], G.S.F.Stephans[9], T.Tamagawa[10], M.J.Tannenbaum[2], J.H.Thomas[2], S. Ueno-Hayashi[11], F.Videbæk[2], F.Wang[17], Y.Wu[17], H.Xiang[4], G.H.Xu[4], K.Yagi[11], H.Yao[9], W.A.Zajc[17], F.Zhu[2]

E917 Collaboration
B.Back[1], R.R.Betts[1,7], H.Britt[13], J.Chang[4], W.C.Chang[4], C.Y.Chi[17], Y.Chu[2], J.Cumming[2], J.C.Dunlop[9], W.Eldredge[4], S.Y.Fung[4], R.Ganz[7], E.Garcia[13], A.Gillitzer[1], G.Heintzelman[9], W.Henning[1], D.Hofman[1], B.Holzman[7], J.H.Kang[12], E.J.Kim[12], S.Y.Kim[12], Y.Kwon[12], D.McLeod[7], A.Mignerey[13], M.Moulson[17], V.Nanal[1], C.A.Ogilvie[9], R.Pak[14], A.Ruangma[13], D.Russ[13], R.Seto[4], J.Stanskas[13], G.S.F.Stephans[9], H.Q.Wang[4], F.Wolfs[14], A.Wuosmaa[1], H.Xiang[4], G.H.Xu[4], H.Yao[9], C.Zou[4]

[1] Argonne National Laboratory, [2] Brookhaven National Laboratory, [3] University of California, Space Sciences Laboratory, Berkeley, [4] University of California, Riverside, [5] High Energy Accel. Res. Organization (KEK), [6] High Energy Accel. Res. Organization (KEK), Tanashi-branch, [7] University of Illinois at Chicago, [8] Lawrence Livermore National Laboratory, [9] Massachusetts Institute of Technology, [10] Department of Physics, University of Tokyo, [11] University of Tsukuba, [12] Yonsei University, [13] University of Maryland, [14] University of Rochester, [15] Center for Nuclear Study, School of Science, University of Tokyo, [16] Oak Ridge National Laboratory, [17] Columbia University

Particle production and correlation functions from Au+Au reactions have been measured as a function of both beam energy (2-10.7AGeV) and impact parameter. These results are used to probe the dynamics of heavy-ion reactions, confront hadronic models over a wide range of conditions and to search for the onset of new phenomena.

1. INTRODUCTION

Very dense nuclear matter is formed in Au+Au collisions at beam energies near 10 AGeV. The physics of such dense matter is intriguing - whether the system behaves as an interacting mixture of excited hadronic resonances, or whether the density is sufficiently high that some of the matter is converted to deconfined quarks and gluons.

Experiments E866 and E917 at the AGS aim to characterize as fully as possible the emission of particles from Au+Au collisions to probe the properties of such dense matter. In Quark Matter '96[1] the E866 collaboration reported that the proton rapidity distribution for central collisions is peaked at mid-rapidity[2]. This is consistent with forming a dense, baryon-rich system. The dynamics of this system were further characterized by the spectra and yield of the most abundantly produced particles, pions and kaons. These results are summarized here for reference. The measured mid-rapidity K^+/π^+ ratio in central reactions is 0.19±0.01. This continues a steady increase in the K^+/π^+ ratio from p+A[3] and Si+A[4] reactions. The transverse m_t spectra of different particles have different spectral shapes, with an overall trend that the proton spectra have larger inverse slopes than the kaon spectra, which in turn have larger inverse slopes than the pion spectra. Detailed analysis[1,2] revealed that the π^- transverse spectra have a low p_t rise above an exponential that is steeper than the rise in π^+ spectra. Such features originate from the interplay between multiple collisions of hadrons, expansion of the system, decay of resonances and Coulomb effects.

Since Quark Matter '96, the E866 and E917 collaborations have continued to work on several open questions, two of which will be the main topics of this paper; 1) is there any evidence for new physics beyond hadronic multiple collisions, for example the formation of a baryon rich quark-gluon plasma? and 2) is the collision zone at thermal equilibrium? These questions are linked because a high collision rate will drive the system towards equilibrium and also alter the signatures of a possible quark-gluon plasma that might be formed early in the reaction.

2. EXPERIMENT

The results in this talk come from two separate collaborations, E866 and E917, that used much of the same equipment. Experiment E866 measured Au+Au reactions at 2, 4, and 10.7 A GeV kinetic energy. Experiment E917 also measured Au+Au reactions but at 6, 8 and 10.7 A GeV kinetic energy. Experiment E866 consists of two magnetic spectrometers that rotate independently. The Forward spectrometer was used only in E866 and was optimized for tracking in the high-multiplicity forward region. This 6msr spectrometer consists of a sweeping magnet followed by two tracking stations before and after a dipole magnet. Each tracking station is a TPC placed between high resolution drift chambers. Particle identification is performed with a TOF-wall with 70ps timing resolution. The older spectrometer, Henry Higgins, has an acceptance of 25msr and was used by both E866 and E917. It consists of drift chambers on either side of a dipole magnet. Particle identification is performed with a TOF-wall with a timing resolution of 130ps. The Henry Higgins spectrometer has an on-line particle identification trigger. Both experiments used the same detectors for global characterization of the events: a multiplicity counter surrounding the target, and a calorimeter placed at zero degrees with

a 1.5^o opening angle. E917 added a beam-vertexing detector to improve the reaction plane measurement. The total systematic uncertainty in the normalization of the cross-sections is 15% and the systematic uncertainty on the inverse slope parameters is estimated to be 5%. For more details on the equipment and data analysis the reader is referred to references[2,5].

3. EXCITATION FUNCTION

Measurement of an excitation function can provide more insight into the mechanism of particle production than results at a single beam energy. An excitation function can also confront hadronic cascade models over a wider range of conditions and thus permit a search for the onset of any new phenomena, e.g. the formation of a small volume of a baryon-rich QGP.
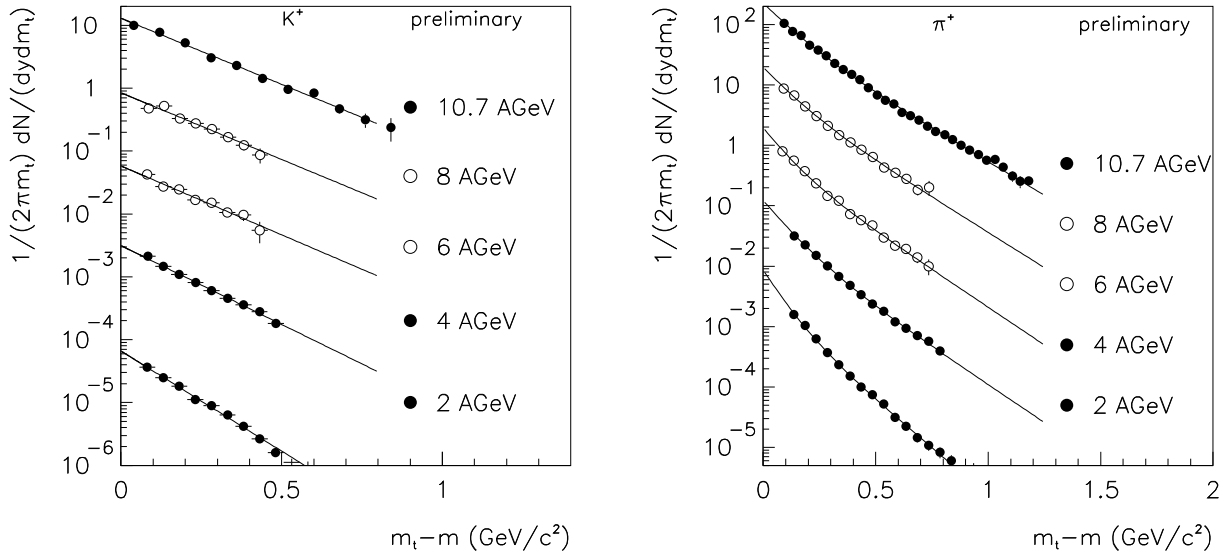

Figure 1. The invariant yield of K^+ (left panel) and π^+ (right panel) per event as a function of m_t at mid-rapidity for the different beam energies. The data from E866 are shown as filled circles and the data from E917 are shown as open circles. The data at 10.7AGev are shown at the correct scale, the data at each lower energy are divided by ten for clarity. The errors are statistical only.

Kaon production is a sensitive probe of hadronic multiple collisions in heavy-ion reactions and may also provide evidence for the formation of a QGP. The left panel of Figure 1 shows a plot of the invariant yield of kaons as a function of transverse mass, $m_t = \sqrt{p_t^2 + m_0^2}$, produced in Au+Au central collisions at 2, 4, 6, 8, and 10.7 AGeV kinetic beam energy. The centrality selection at each beam energy was the inner 8% of the total interaction cross-section (σ_{int}=6.8b). Each spectrum covers the mid-rapidity range corresponding to that beam energy, $|\frac{y-y_{nn}}{y_{nn}}| < 0.25$. The kaon spectra were fit with an exponential function in m_t. The fits reproduce the spectra well and provide the inverse slope parameter T and the rapidity density, dN/dy, in that rapidity slice.

4

The right panel of Figure 1 shows the invariant spectra for π^+ from Au+Au reactions at each of the five beam energies. The pion spectra rise at low p_t above an exponential. These spectra have therefore been fitted with a double exponential, with the dN/dy and mean m_t as two of the fit parameters.

The mid-rapidity yields of π^+ and K$^+$ as a function of the initial available energy $\sqrt{s}$ are shown in the upper panels of Figure 2. Both pion and kaon yields increase steadily
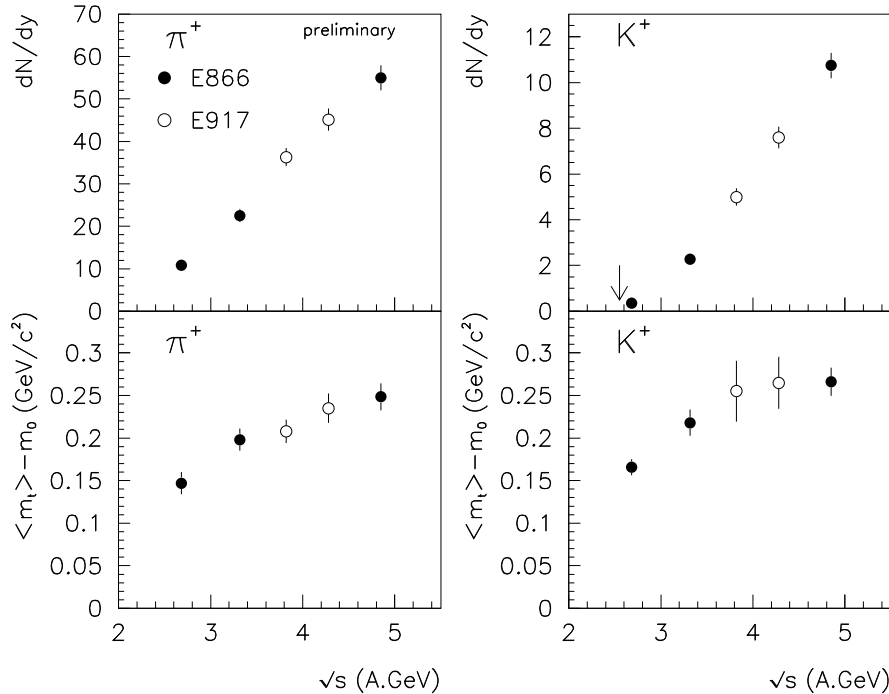

Figure 2. The yield of π^+ and K$^+$ at mid-rapidity (top-panels) for central Au+Au reactions as a function of the initial available beam energy. The lower panels show the mean m_t minus the rest mass for π^+ and K$^+$ at the same rapidity. The arrow indicates the N-N threshold for K$^+$ production. The errors include both statistical and a 5% point-to-point systematic uncertainty.

and smoothly with beam energy. There is no indication of any sudden increase in particle yield with increasing $\sqrt{s}$. In the lower panels of Figure 2, the mean m_t of the transverse spectra for pions and kaons are plotted versus $\sqrt{s}$. Compared to the increase of particle production, the mean m_t increases slowly with beam energy. The extra available energy mainly goes into more particle production rather than increased transverse energy.

The increase in kaon yield with beam energy is more rapid than the increase of pion yield. This is emphasized in Figure 3, where the K^+/π^+ ratio is plotted versus $\sqrt{s}$. This ratio increases steadily from near 3% at 2 AGeV to 19% at 10.7 AGeV.

These extensive measurements over a broad range of conditions provide a stringent test of hadronic models. The predictions of the RQMD hadronic cascade[6] have been compared to the measured ratio K^+/π^+ (Figure 3). The model reproduces the data well.

It is however hard to distill any simple physics lesson from a comparison with such a complicated model. One way to improve our understanding is to divide the Au+Au
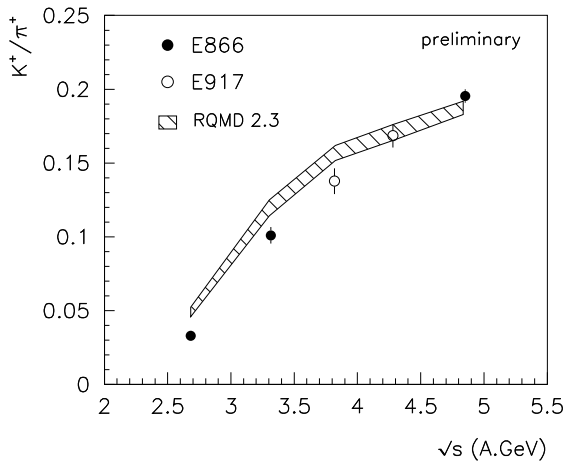
Figure 3. The ratio K^+/π^+ at mid-rapidity in central Au+Au reactions as a function of the initial available energy. The errors are statistical only.
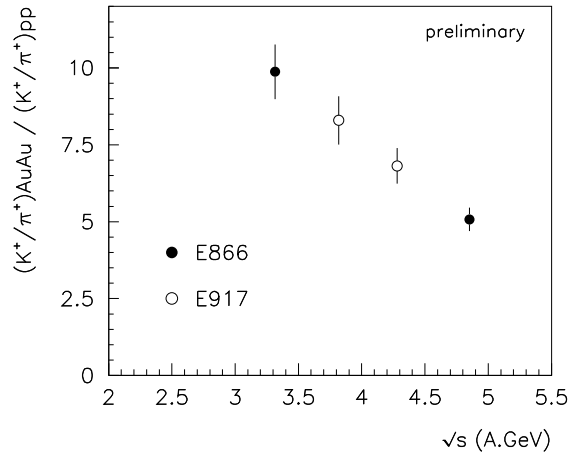
Figure 4. The double ratio K^+/π^+ at mid-rapidity from central Au+Au reactions divided by K^+/π^+ of total yields from p+p reactions as a function of the initial available energy. The errors include both statistics and a 5% systematic uncertainty in the K/π ratio from p+p reactions.

K^+/π^+ ratio by the K^+/π^+ ratio from p+p reactions[7–9] (Figure 4). This double ratio is greater than one, demonstrating that K/π is enhanced in Au+Au reactions relative to p+p collisions. This enhancement is largest at the lowest beam energy, possibly because secondary collisions increase in relative importance compared to initial collisions as the beam energy is reduced. At the kaon threshold this double ratio goes to infinity[10]. Also note that the double ratio at 2GeV is not plotted because of the large uncertainty in the p+p kaon yield.

4. CENTRALITY DEPENDENCE

At each beam energy the experiment was triggered primarily with spectrometer-based triggers. The spectrometer data can then be sorted off-line into several centrality classes. At this stage of the analysis, results are only available for the centrality dependence of particle production at the full energy, 11.6 A GeV/c, from Experiment E866.

As the reactions become more central, the number of primary and secondary hadron-hadron collisions increase. By measuring particle spectra and yields as a function of centrality we probe how these collisions affect particle production. In addition, because the volume of dense nuclear matter increases with centrality[11], we can search for the onset of any new phenomena associated with high densities.

The measured energy near zero degrees (E_{ZCAL}) is dominated by projectile spectator nucleons and provides an estimate of the initial overlap of the projectile and target nuclei. The number of projectile participants, N_{pp}, is estimated from the measured E_{ZCAL}

$$N_{pp} = 197 \times (1 - E_{ZCAL}/E_{beam}^{kin}) \tag{1}$$

where E_{beam}^{kin}=2123 GeV is the kinetic energy of the beam. The event classes are defined by cuts in E_{ZCAL}. These are referenced by their cross-section: 0-5%, 5-12%, 12-23%, 23-39% and 39-73% of the total interaction cross-section, σ_{int}=6.8b.
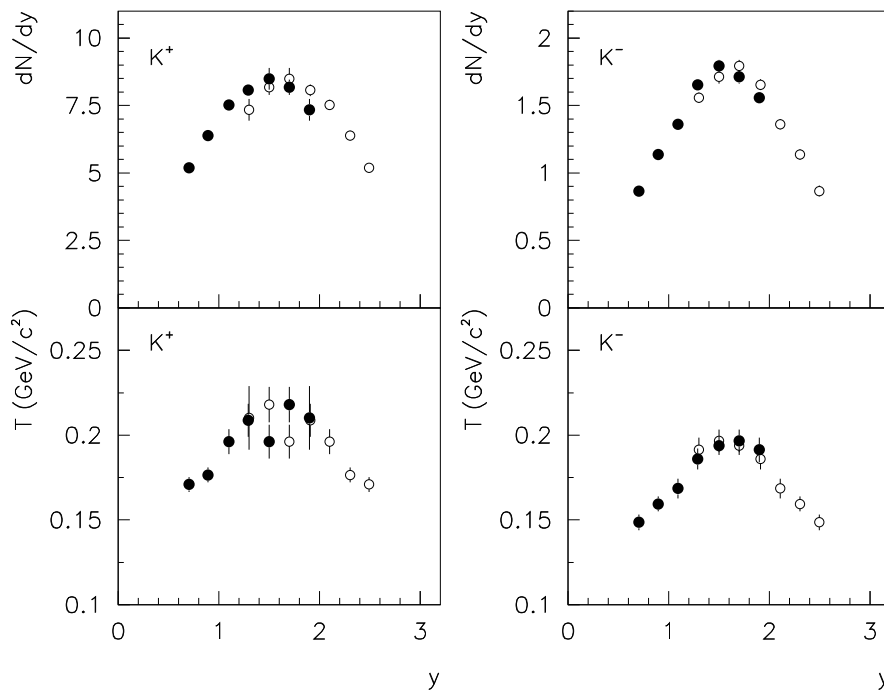

Figure 5. The dN/dy and inverse slope distributions as a function of rapidity for K^+ and K^- emitted from mid-central Au+Au reactions at 11.6 A GeV/c. The errors are statistical only. The hollow circles are the data points reflected about mid-rapidity (y=1.6).

In the top panels of Figure 5, dN/dy distributions for K^+ and K^- are shown for the 5-12% event class of Au+Au reactions at 11.6 AGeV/c. These have been extracted from fits to invariant spectra as a function of transverse mass, similar to those shown in Figure 1. Also extracted from each transverse spectrum is the inverse slope, T. The rapidity dependence of the inverse slope parameter is shown in the lower panels of Figure 5. Both the dN/dy and the inverse slope distributions peak at mid-rapidity. The dN/dy distribution for K^- is narrower than for K^+, and the K^+ inverse slopes tend to be slightly larger than the inverse slope for K^-.

To extract the total yield of kaons per event, each dN/dy distribution was fitted with a Gaussian centered at mid-rapidity (y=1.6) In Figure 6, the K^+ yield is plotted as a function of the number of projectile participants. The yield of K^+ increases non-linearly with N_{pp}, implying that kaon production is more efficient in central collisions. This is emphasized in the middle panel of Figure 6, where the K^+ yield per participant is plotted. The yield of kaons per participant in central reactions is 3.5 times the yield from isospin-averaged N-N collisions at the same beam energy[8,9]. This suggests that the majority of kaons in central reactions are produced by secondary collisions.

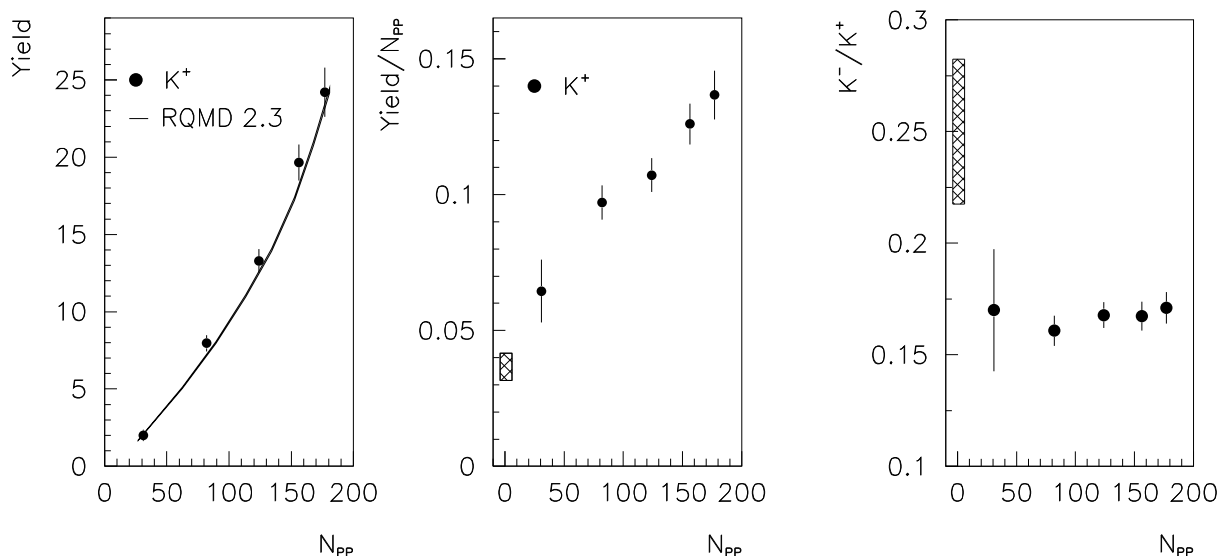The hadronic cascade model, RQMD[6], attempts to simulate how these secondary col-

Figure 6. Left panel: the average yield of kaons in an event as a function of the number or projectile participants in Au+Au reactions at 11.6 A GeV/c. Middle panel: the yield of K^+ per projectile participant. Right panel: The ratio of the total yields of K^- and K^+ as a function of the number of projectile participants. The errors are statistical only. The hatched boxes are the yields from the isospin averaged initial N-N collisions.

lisions occur in a heavy-ion reaction. The model reproduces both the absolute magnitude of kaon production and the dependence of yield on the number of projectile participants quite well.

The yields of π^+, π^-, K^-, and $\overline{p}$ have also been measured as a function of centrality. The right panel of Figure 6 shows the ratio of total yields K^- to K^+. This ratio is strikingly constant over the measured range of centrality and below the estimated K^-/K^+ ratio from initial N-N collisions[8,9]. The K^- yield increases non-linearly with N_{pp} in a manner very similar to the K^+ yield. This is surprising since the two particles have different underlying production mechanisms, energy thresholds and absorption rates.

The observation that the K^-/K^+ ratio is independent of centrality may also test models that include an in-medium mass for kaons. There have been several predictions that the K^- mass decreases with increasing nuclear density [12–14]. Such a conjecture could lead to more phase space for K^-+K^+ pair production which would increase the K^-/K^+ ratio in central reactions. This is not observed, potentially placing a constraint on the in-medium properties of kaons.

The role of absorption in heavy-ion reaction and how it affects the final yield of particles is perhaps best studied with anti-protons[15]. Figure 7 is a plot of the total yield of $\overline{p}$ per participant as a function of the number of projectile participants. The total yield is from a Gaussian fit to the $\overline{p}$ rapidity distribution measured with the Henry Higgins spectrometer[16].

In contrast to kaon production, the $\overline{p}$ yield per participant is constant and considerably below the N-N value[7]. Both observations are consistent with $\overline{p}$ being strongly absorbed.

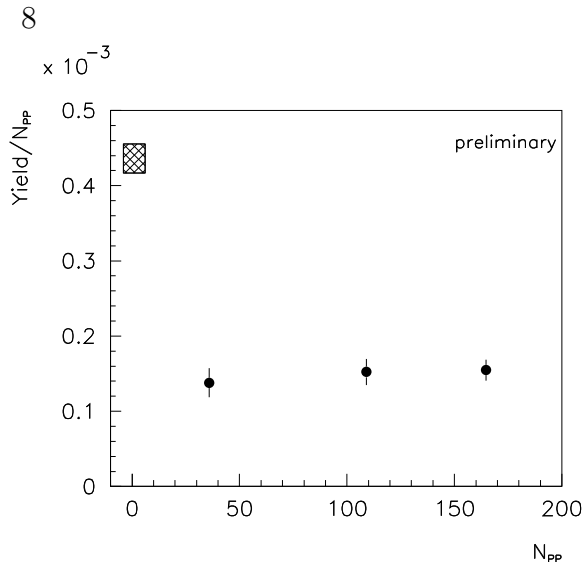The final yield of $\overline{p}$ is sensitive not only to absorption but also to the extent that

Figure 7. The yield of $\overline{p}$ per participant as a function of the number of projectile participants in Au+Au reactions at 11.6 A GeV/c. The errors are statistical only. The box on the left is the estimated yield from the initial N-N collisions.
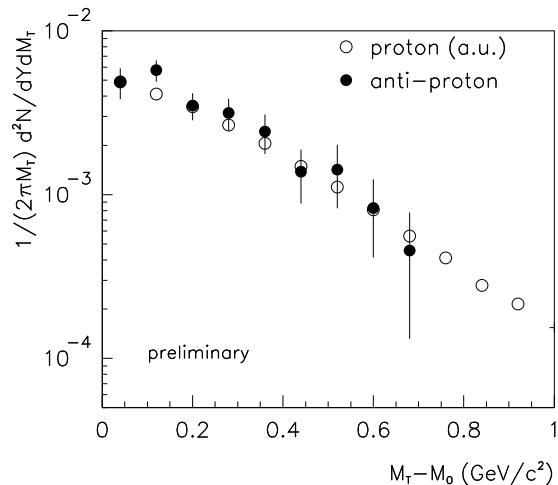
Figure 8. The invariant spectrum of $\overline{p}$ at mid-rapidity as a function of transverse mass in Au+Au reactions at 11.6 A GeV/c. For comparison the proton spectrum at the same rapidity is also shown. The errors are statistical only.

secondary collisions enhance $\overline{p}$ production. Extra information to help disentangle these two effects may come from the transverse spectra of $\overline{p}$. The mid-rapidity spectrum of $\overline{p}$ as measured with the Forward-spectrometer[16] in central Au+Au reactions is shown in Figure 8. For comparison the proton spectrum is shown on the same plot arbitrarily normalized to the $\overline{p}$ yield at low m_t. Within the current statistics these two spectra have a similar shape. This is a puzzle since $\overline{p}$ produced at low m_t should be strongly absorbed, which would effectively increase the inverse slope parameter. This effect may, however, be counterbalanced by the low phase space available for $\overline{p}$ production which effectively reduces the inverse slope parameter.

5. PION INTERFEROMETRY

The interference of identical particles (HBT) provides additional information on the dynamics of heavy-ion reactions and on the space-time extent of particle emission. Experiment E866 has two parallel efforts in this field; 1) to map out the systematic evolution of the HBT source parameters with changing initial system size, from peripheral Si+A reactions to central Au+Au collisions, and 2) to probe the reaction dynamics by extracting HBT parameters as a function of the momentum of the particles[17,18]. Only the first aspect of our efforts will be reported here.

Experiments E859 (Si+A) and E866 (Au+Au) have measured the systematic evolution of HBT interferometry for identical pions. This comprehensive data set establishes how the extracted HBT parameters vary as a function of the initial geometry of the reaction. Any change in this relationship may indicate the onset of new phenomena, e.g. a change in expansion driven by forming a small volume of baryon-rich QGP[19–21].

Each pion two-particle correlation function is measured in three dimensions corresponding to the three components of relative momentum[19,20]: q_z is parallel to the beam, q_{tout} is parallel to the sum of the transverse momenta of the pair and q_{tside} is in the orthogonal transverse direction. The correlation functions were fit with the following Gaussian.

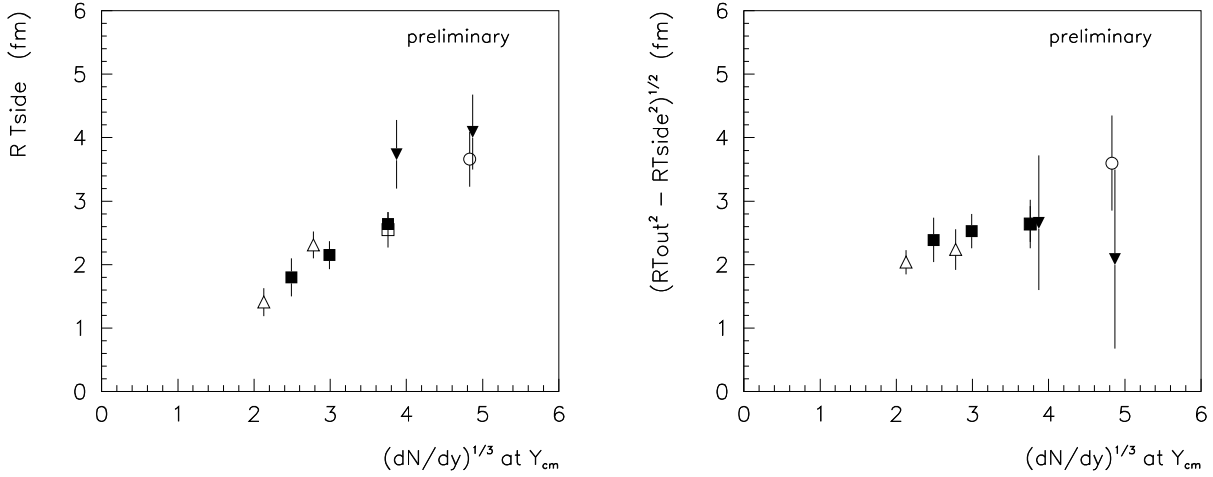$$C(q) = 1 + \lambda e^{-((R_{tout}q_{tout})^2 + (R_{tside}q_{tside})^2 + (R_z q_z)^2)/2} \tag{2}$$

Figure 9. The extracted parameter R_{tside} (left panel) and the quadratic difference of R_{tout} and R_{tside} (right panel) versus the cube-root of the total pion dN/dy. E859 Si+Al, Si+Au results are shown as open triangles and filled squares respectively. E866 Au+Au results are shown as open circles and filled inverted triangles. The errors are statistical only.

The extracted parameter R_{tside} is primarily sensitive to the transverse geometry and dynamics of the source. In the left panel of Figure 9, R_{tside} shows a steady, linear increase with the cube-root of the pion rapidity density. There is no anomalous increase that would indicate a rapid change in the size of the emitting system or a change in its expansion dynamics.

The quadratic difference of R_{tout} and R_{tside} (right panel of Figure 9) is sensitive to both the duration of emission of the source and its dynamics[19,20]. In contrast to R_{tside}, the quadratic difference is independent of the initial system size. This is consistent with the duration of emission being similar for all the systems studied.

6. TESTS OF EQUILIBRIUM

It is possible that information from an early, small, volume of QGP may be lost in the randomizing collisions during the hadronic phase. Inelastic collisions alter the signatures of particle abundances and all collisions alter the kinematic signatures. A system with a high collision rate will be driven towards thermal equilibrium and potentially lose information about a possible QGP. To assess this possibility, we need to quantify how close the emitting system is to thermal equilibrium.

As observed earlier in this paper, the rapidity distributions for K^+ and K^- are different. This is emphasized in Figure 10 which shows the K^-/K^+ ratio as function of rapidity for

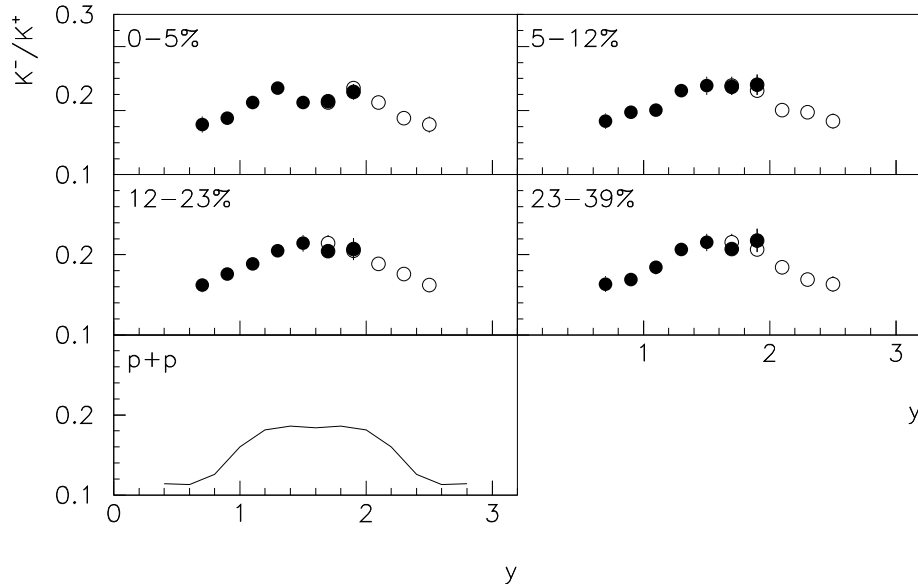different centrality classes in Au+Au reactions at 11.6 A GeV/c. The rapidity distribution

Figure 10. The ratio of the the K^- and K^+ dN/dy distributions for different centrality classes in Au+Au reactions at 11.6 A GeV/c. The errors are statistical only. The lower panel is for p+p reactions at 12 GeV/c and is adapted from Fesefeldt et al. [8].

for K^- is narrower than the K^+ distribution for all centralities and also for p+p reactions at 12 GeV/c. This is consistent with K^- having less phase space than K^+ due to a higher energy threshold for K^- production.

Figure 11 shows the difference between the inverse slopes from K^+ and K^- transverse spectra as a function of rapidity for each centrality class in Au+Au reactions at 11.6 A GeV/c. Systematically the K^+ inverse slopes are 10 to 20 MeV larger than the K^- inverse slopes. The difference in inverse slopes is consistent with less phase space available for K^- production.

The fact that K^+ and K^- have different rapidity distributions and transverse spectra excludes a commonly used class of thermal models[23], namely those models that assume that thermal parameters are uniform across the emitting system and that all particles are in kinetic equilibrium. For a system at kinetic equilibrium, there is sufficient scattering so that the spectra of equal mass particles are identical in shape, even if the system is expanding. It may however be possible to reconcile these data with a modified thermal model, either with a rapidity-dependent chemical potential or temperature, or possibly different freezeout conditions for K^- and K^+.

The comparison between the K^+ and K^- spectra may also constrain and test hadronic models that include in-medium properties of kaons. The effects of a reduced kaon mass are often modeled by an attractive kaon mean-field[13,14]. This would pull K^- particles to lower m_t and reduce the inverse slope parameter. The repulsive mean-field for K^+ should increase the inverse slope parameter. Because the mean-fields are predicted to increase with density, the difference in kaon spectral shapes might be expected to grow for more central reactions. This is not observed.
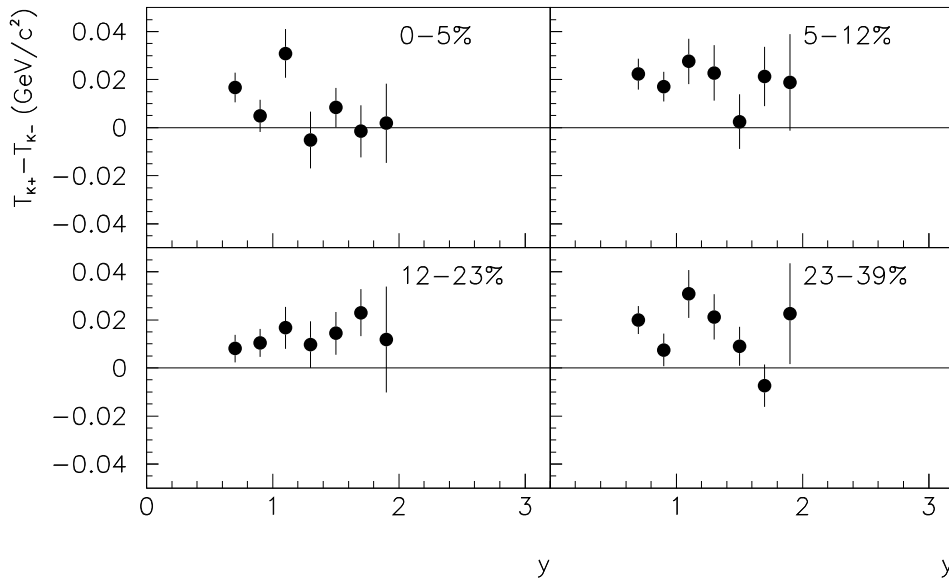
Figure 11. The difference between the K$^+$ and K$^-$ inverse slope parameters as a function of rapidity for different centrality classes in Au+Au reactions at 11.6 A GeV/c. The errors are statistical only.

7. Summary of Results and Conclusions

By mapping out the evolution of the spectra, yields and correlation functions of produced particles, we have probed the effects of multiple hadronic collisions, absorption, and energy thresholds in heavy-ion reactions. Across the broad systematic data set there is no evidence for any onset of new behavior beyond hadronic scattering as the beam energy or centrality is changed. There are however three outstanding puzzles; 1) why is the ratio of yields K$^-$/K$^+$ independent of centrality, 2) why do the transverse spectra of $\overline{p}$ and protons have similar shapes, and 3) why is the quadratic difference of R$_{tout}$ and R$_{tside}$ constant?

One of the largest puzzles in AGS physics is that hadronic models[6,11,22] predict that a small region of very dense nuclear matter ($\rho > 8\rho_0$) exists during an Au+Au collision, but no evidence for a QGP has been observed. There are two possibilities: 1) a baryon-rich QGP is not formed in such a region or is very small, 2) the information from such a plasma is lost after hadronization by the many hadronic collisions. The second possibility makes it difficult to set a quantitative limit on QGP formation. To do so will require a model-dependent study of inserting an ad-hoc change into the particle distributions during the model evolution of a heavy-ion reaction. How much information is retained from this disturbance provides an estimate of the survivability of QGP signatures. This clearly depends on how frequent the collisions are in the hadronic phase. The measured spectral differences between K$^+$ and K$^-$ can be used to test the assumptions of hadronic collision rates in such a study.

Experimentally, the challenge is to extend the results to more sensitive probes, such as the yield of $\overline{\Lambda}$, ϕ, and also to extend our studies to more exclusive variables, e.g. the azimuthal distribution of particle production with respect to the reaction plane. It will

also be important to increase the range of observables included in the excitation function to proton stopping via the proton rapidity distributions, as well as to the rapidity and m_T dependence of HBT source parameters.

REFERENCES

1. L. Ahle et al., Nucl. Phys. A610 (1996) 139c.
2. L. Ahle et al., E866 Collaboration Phys. Rev. C57 vol2 (1998).
3. T. Abbott et al., Phys. Rev. D 45 (1992) 3906.
4. T. Abbott et al., Phys. Rev. C 50 (1994) 1024.
5. T. Abbott et al., Nucl. Instrum. Methods A290 (1990) 41.
6. H. Sorge, H. Stöcker and W. Greiner , Ann. Phys. (NY) 192 (1989) 266.
7. A.M. Rossi et al., Nucl. Phys. B84 (1975) 269.
8. H. Fesefeldt et al., Nucl. Phys. B147 (1979) 317.
9. V. Blobel et al., Nucl. Phys. B69 (1974) 454.
10. Fermi motion in Au will also increase the K/π double ratio but Fermi motion cannot account for the increased K/π ratio observed as a function of centrality.
11. B-A. Li and C.M. Ko, Phys. Rev. C **52**, 2037 (1995).
12. W. Weise, Nucl. Phys. A610 (1996) 35c.
13. B.-A. Li and C.M. Ko, Phys. Rev. C 54 (1996) 3283.
14. W. Ehehalt and W. Cassing, Nucl. Phys. A602 (1996) 449.
15. A. Jahns et al., Phys. Rev. Lett. 68 (1992) 2895.
16. The $\overline{p}$ have not been corrected for feed-down from $\overline{\Lambda}$ decay. For the Henry Higgins and Forward spectrometers the acceptance for daughter $\overline{p}$ from $\overline{\Lambda}$ decay is approximately 100% and 65%, respectively.
17. U. Heinz, Nucl. Phys. A610 (1996) 264c
18. H. Beker et al., NA44 Collaboration, Phys. Rev. Lett. 74 (1995) 3340.
19. G. Bertsch Nucl. Phys. A498 (1989) 173c.
20. S. Pratt et al., Phys. Rev. C42 (1990) 2646.
21. D. Rischke Nucl. Phys. A610 (1996) 88c.
22. Y. Pang, T.J. Schlagel, and S.H. Kahana, Phys. Rev. Lett. **68**, 2743 (1992).
23. P. Braun-Munzinger et al., Phys. Lett. **B344** 43 (1995).